iScience

CellPress
OPEN ACCESS

Article

Observation of induction period and oxygenated intermediates in methane oxidation over Pt catalyst

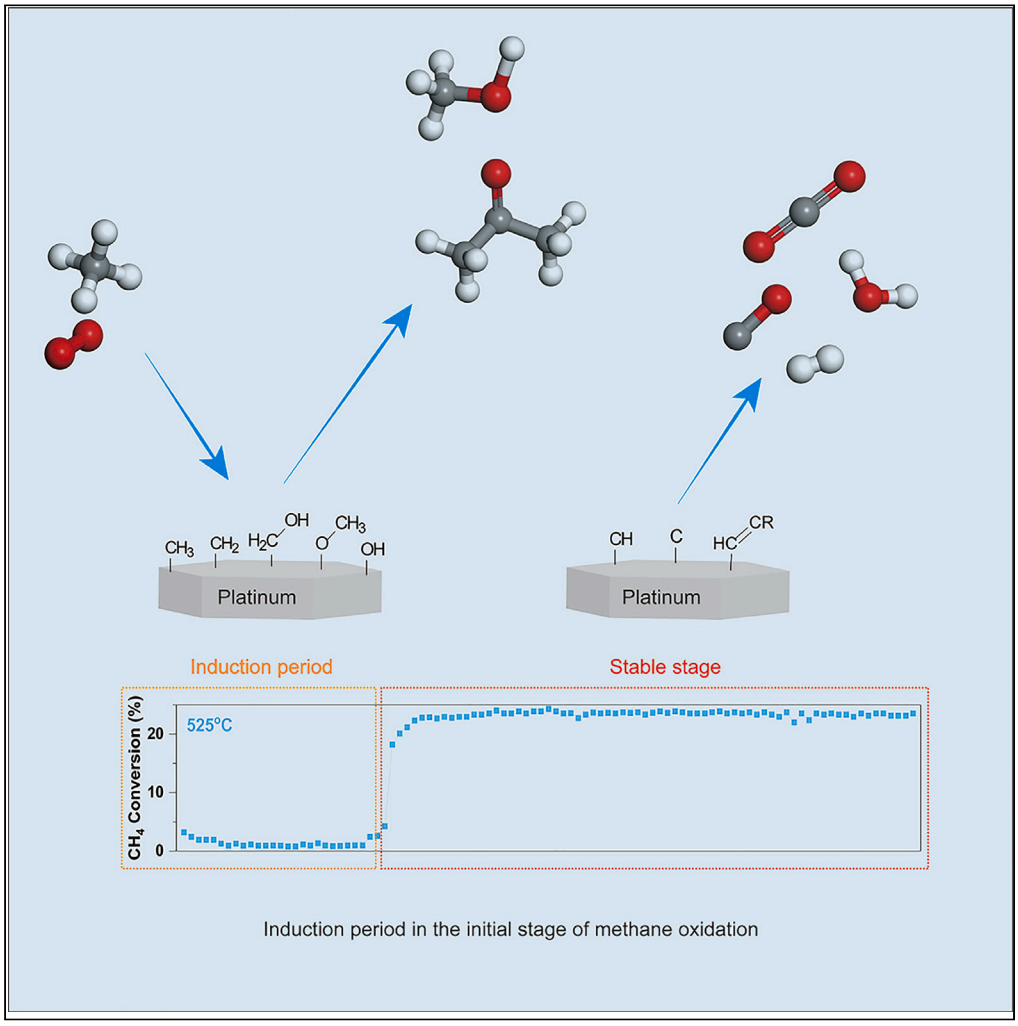

Induction period in the initial stage of methane oxidation

Kuo Yang, Jinzhe Li, Zhongkui Zhao, Zhongmin Liu

zkzhao@dlut.edu.cn (Z.Z.)
liuzm@dicp.ac.cn (Z.L.)

Highlights

An induction period is observed at the initial stage during methane oxidation

Multiple oxygenated intermediates are detected during the induction period

Induction period can be shortened by active species formed by methane pretreatment

The mechanism for methane oxidation over platinum is proposed

Yang et al., iScience 26, 107061
July 21, 2023 © 2023 The Author(s).
https://doi.org/10.1016/j.isci.2023.107061

iScience

CellPress
OPEN ACCESS

Article

Observation of induction period and oxygenated intermediates in methane oxidation over Pt catalyst

Kuo Yang,[1,2] Jinzhe Li,[2] Zhongkui Zhao,[1,*] and Zhongmin Liu[2,3,4,*]

SUMMARY

Selective oxidation of methane is one of the most attractive routes for methane to chemicals. However, mechanistic understanding and avoiding over-oxidation have great challenges because of its very rapid reaction rate. Herein, a capillary micro-reaction system was introduced to monitor the initial stage of methane oxidation over platinum. For the first time, an induction period is observed, during which oxygenated intermediates, such as methanol, acetone, methyl methoxy acetate, etc., are detected. Induction period can be shortened by methane pretreatment at 600°C, which generates highly active species containing unsaturated bonds. Combined these findings and observations of *in situ* characterizations, the evolution route of methane oxidation over Pt is prosed, i.e., the reaction starts from the formation of initial species containing Pt-C bond, followed by the generation of oxygenated intermediates, and ended with the over-oxidation of the intermediates to CO/CO_2.

INTRODUCTION

Methane, the predominant component of natural gas, is a high-profile source of energy and C1 feedstock for producing numerous downstream chemicals.[1–3] Direct and indirect routes of methane conversion have received intense attention for many decades. Among these routes, methane direct oxidation by oxygen is the most expected one for producing chemicals. However, because of the very rapid reaction rate, mechanistic understanding and further controlling of the reaction to avoid over-oxidation of the chemical intermediates and products have been great challenges for long time. Commercially, the indirect route through conversion of methane to synthesis gas ($CO + H_2$) following with further transformation to value added products is still the main way for the application of methane as chemical feedstock.[4,5]

A significant amount of research has been aimed at exploring fundamental mechanism and practical aspects associated with catalytic partial oxidation (CPOX) of methane. Almost all transition metal catalysts have been investigated,[6–12] whereas most of them suffer from low efficiency. Compared with non-noble metal catalysts, noble metals such as platinum and palladium exhibit great potential for commercial implementation ascribed to the lower activation barrier of O-O and C-H bonds, low-temperature activity, coking resistance, as well as high-temperature adaptability.[13–16] Major focuses of the previous studies were on CH_4-O_2 and CH_4-H_2O/CO_2 reaction systems and the reaction mechanisms are mainly classified into two categories: direct mechanism and indirect mechanism. The direct mechanism considered H_2 and CO directly generated by CH_4-O_2 reactants.[17–20] In contrast, the indirect mechanism proposed that CH_4 molecules were completely oxidized to CO_2 and H_2O as first step and then following with steam reforming and dry reforming reactions.[15,21–24] However, the discrimination between the direct and the indirect mechanism is very difficult because of the complexity of the reaction system involving intrinsic reaction and mass transfer, and being strongly affected by reaction conditions and the presence of concentration and temperature gradients within packed-beds or on catalysts. As oxidation reaction of CH_4 and related organic species is always extremely rapid, it is very difficult to capture the intermediate species and follow their mechanism variations with normal reaction method.

Herein, we introduce a capillary micro-reaction system connecting online mass spectrometer and online chromatograph which enables to monitor the reaction progress at very short contact time (≤1 ms) and in the initial stage of the methane oxidation reaction. Both pulse injection and continuous flow experiments

[1]State Key Laboratory of Fine Chemicals, Department of Catalysis Chemistry and Engineering, School of Chemical Engineering, Dalian University of Technology, Dalian 116024, China

[2]National Engineering Research Center of Lower-Carbon Catalysis Technology, Dalian National Laboratory for Clean Energy, Dalian Institute of Chemical Physics, Chinese Academy of Sciences, Dalian, Liaoning 116023, China

[3]University of Chinese Academy of Sciences, Beijing 100049, China

[4]Lead contact

*Correspondence: zkzhao@dlut.edu.cn (Z.Z.), liuzm@dicp.ac.cn (Z.L.)

https://doi.org/10.1016/j.isci.2023.107061

This is an open access article under the CC BY-NC-ND license (http://creativecommons.org/licenses/by-nc-nd/4.0/).

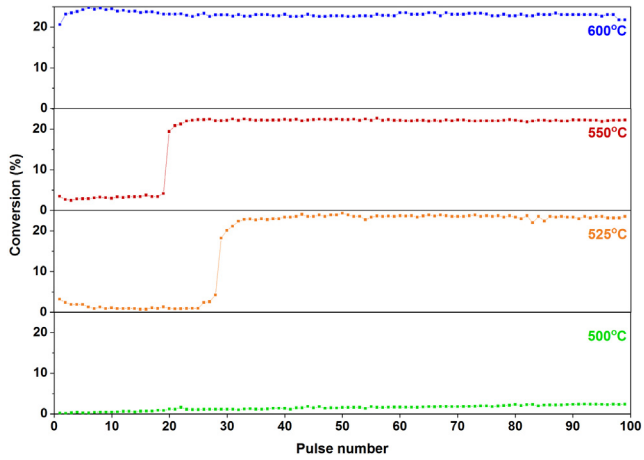

Figure 1. CH_4 conversion as a function of O_2 pulse number (99)

Reaction conditions: pulse injection mode, p = 1 bar, CH_4/O_2 = 2, contact time = 1 ms, pulse interval = 0.15 min, pulse number = 99.

were carried out to investigate the reaction behavior at various reaction conditions. Unlike traditional reaction manner, the specially designed capillary reactor with platinum wires catalyst also accelerates mass transfer and facilitates heat transfer over the catalyst, which greatly reduces the concentration and temperature gradients within the catalyst bed. Moreover, owing to the limited number of dispersed Pt surface atoms on Pt wires, the concentration gradients of adsorbed species along the catalyst bed can also be avoided. This provides a new feasible tool to follow the evolution of intermediate species and a further understanding of the mechanism of rapid reactions such as CH_4 oxidation.

RESULTS AND DISCUSSION

Induction period of methane oxidation

The capillary reaction system is described in method details section. The pulse injection mode was used to investigate the initial stage of methane oxidation at very short contact time ($\leq$1 ms). Before that, the blank experiments without catalyst were conducted at the temperature range of 500°C–800°C and no CH_4 oxidation was observed (Figure S1). The results of CH_4 oxidation over Pt wires at different temperature were shown in Figures 1, 2, S2, and S3.

The temperature has very important effect on the pulse reaction. At 500°C, CH_4 conversion (Figure 1) was quite low (0.1–2.4%) and gas products (Figure S2) were hardly observed during 99 pulses of O_2. When the temperature reached up to 525°C (Figure 1), CH_4 conversion was also very low during the first 26 pulses and a small amount of gas phase products (mainly H_2 and CO_2) were detected. However, at the 27th O_2 pulse, the CH_4 conversion increased sharply and reached to 18.2% with a significantly change of the product distribution, meanwhile the signal of O_2 disappeared (Figure S3). After 29th O_2 pulses, the oxidation reaction reached stable, that is, the CH_4 conversion (~23%) and the distribution of gas products remained relatively constant in the subsequent O_2 pulses. An induction period was clearly observed for CH_4 oxidation at 525°C. A similar induction period of CH_4 conversion was also observed at 550°C, but with relatively less pulses. At 600°C, the first pulse of O_2 resulted in a 20.6% of CH_4 conversion and the induction period could not be observed. The observation of induction period of CH_4 oxidation implies that the surface of the Pt catalyst might undergo some changes during the introduction of CH_4/O_2 which has a remarkable influence on CH_4 oxidation.

To further explore the product evolution during the induction period, the appearing sequence of the reaction products were monitored by the online mass spectrometer and the results are shown in Figure 2. At 525°C, CO_2 was consistently observed as two peaks during each of 26 pulses of O_2 (induction period), indicating that the generation of CO_2 occurs through two different pathways during CH_4 oxidation in the induction period. The first peak of CO_2 appeared relatively independent, at the same time only very weak peaks of H_2, H_2O and CO were observed. This suggests that there should be a change of the Pt surface on

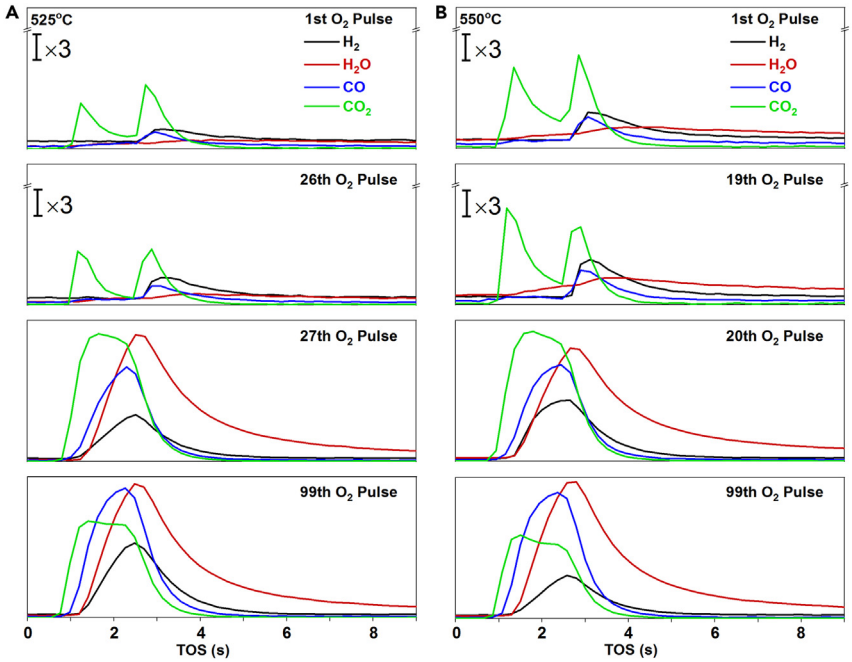

Figure 2. MS spectra signals of gas products during a single O_2 pulse
Reaction conditions: p = 1 bar, CH_4/O_2 = 2, contact time = 1 ms, (A) 525°C, (B) 550°C.

which some hydrogen-rich substances were formed and reserved corresponding to the formation of the first peak of CO_2. These surface substances were formed during the 10 min pre-introduction of CH_4 stream (shown in transparent methods supplemental file). Peaks of H_2, CO and H_2O followed closely with the appearance of second CO_2 peak. The second peak of CO_2 might be partly attributed to the over-oxidation of CO[25] and CH_4 with the adsorbed oxygen on the Pt surface. The generation amount of CO, H_2O and H_2 at the 26th pulse was observed more than that at the first O_2 pulse. At the end of the induction period (27th O_2 pulse), a significant increase in the signals of gas products was observed and the phenomenon of the two CO_2 peaks disappeared. As the reaction gradually reached to a stable state, CO_2 decreased whereas CO increased (99th O_2 pulse). In the case of 550°C reactions, the trend of gas products signals was similar to that of 525°C, except the generation of H_2O in the induction period (1st and 19th O_2 pulse) was significantly higher than that of 525°C, implying that more H atoms dissociated from CH_4 are participated in the reaction with the increase of temperature. The existence of the induction period and the change of the product formation order with increase of the number of O_2 pulses until steady state strongly suggest that there should be corresponding changes of the Pt surface state being closely related to the methane oxidation reaction.

Effect of gas pretreatment on the methane oxidation

To further explore the effect of Pt surface state during the methane oxidation, the Pt wire catalyst was pretreated by different gas (CH_4, H_2 or O_2) at 600°C and then the O_2 pulsing experiments were carried out at 500°C, 550°C and 600°C respectively. Figures 3 and S4 show CH_4 conversion and gas products selectivity as a function of O_2 pulse number, and the MS signals of gas products are shown in Figure S5.

It is evident that the pretreatment with different gases has great influence on the reaction. For O_2 pretreatment, the CH_4 conversion at 500°C was quite low (~1.9%) and only CO and H_2O were detected as gas products. In this case, the oxygen in the form of platinum oxide or chemisorbed oxygen is available, which favors the formation of CO and H_2O. For H_2 pretreatment, the CH_4 conversion at 500°C remained at low values (<5.9%) during 16 O_2 pulses with CO_2 & CO as the main gas products and a small amount of H_2O & H_2. For CH_4 pretreatment, the CH_4 conversion at 500°C exhibited much higher conversion (up to 19.6%) and a shorter induction period (two O_2 pulses), in which CO_2 was observed as the main gas phase product in the initial stage. After the induction period, the selectivity of CO_2 decreased significantly whereas the selectivity of CO and H_2O increased rapidly.

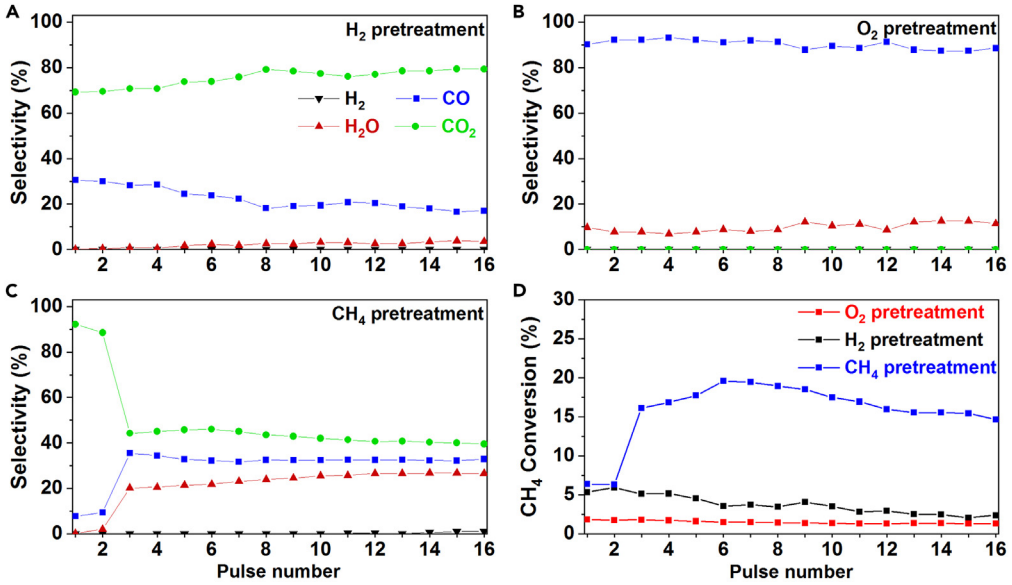

Figure 3. CH_4 conversion and selectivity of gas products as a function of O_2 pulse number at 500°C after pretreatment with O_2, H_2 and CH_4 respectively

Reaction conditions: pulse injection mode, p = 1 bar, CH_4/O_2 = 2, contact time = 1 ms, pulse interval = 16 min, temperature (A) selectivity after H_2 pretreatment, (B) selectivity after O_2 pretreatment, (C) selectivity after CH_4 pretreatment, (D) CH_4 conversion.

As a summary of the above results, the reactions on the catalysts pretreated by O_2 and/or H_2 were still in the induction period and only hydrogen deficient products were observed, whereas the reaction on the CH_4 pretreated catalyst was more easily to overcome the induction period. The different results of H_2 and CH_4 pretreatment indicate that the active species on the two Pt catalysts should be different, though both of them could be expected in reduction states.

With the increase of temperature, the reactivity and products distribution of Pt catalysts after different gases pretreatment were also changed (Figure S4). In the case of O_2 pretreatment, the CH_4 conversion remained at relatively low values (the maximum was 6.2% at 600°C), which indicates the low activity of platinum oxide,[26] and CO_2 became the main product. As for H_2 pretreatment, the conversion increased with temperature, and CO_2 was the main product in the initial stage, but the selectivity of CO and H_2O increased rapidly after the induction period. For CH_4 pretreatment, the CH_4 conversion was higher than that of H_2 pretreatment and almost no induction period was observed (Figures S4A and S4B).

Online gas chromatograph equipped with FID detector were used to detect the effluent products during CH_4 conversion. No detectable products were observed in the blank experiment without catalyst at 500°C–600°C (Figure S6). Figure 4 shows the gas chromatogram of CH_4 conversion at 500°C over pretreated Pt catalyst with different gas pretreatment. Methanol (Rt 8.5 min), acetaldehyde (Rt 9.6 min), acetone (Rt 13.5 min) and methyl methoxyacetate (Rt 15.1 min) were detected in the effluent of CH_4 conversion over all of the three catalysts. Especially, methyl methoxyacetate appeared in second O_2 pulse and disappeared in third pulse. The transient existence of methyl methoxyacetate indicates that the corresponding changes of the Pt surface state also being closely related to the distribution of oxygenated compounds. The methoxy group in methyl methoxyacetate suggests the interaction of hydrogen-rich substances with O_2 might generate the methoxy group over Pt surface. Furthermore, these oxygenated compounds were also detected during CH_4 conversion at 550°C and 600°C (Figure S7). However, the amount of oxygenated compounds was still too small to analyze quantitatively.

Study on the oxygenated intermediates during methane oxidation

Because the amount of oxygenated compounds was too small to analyze quantitatively in the pulse injection mode, the continuous feed mode was employed to systematically investigate these oxygenated

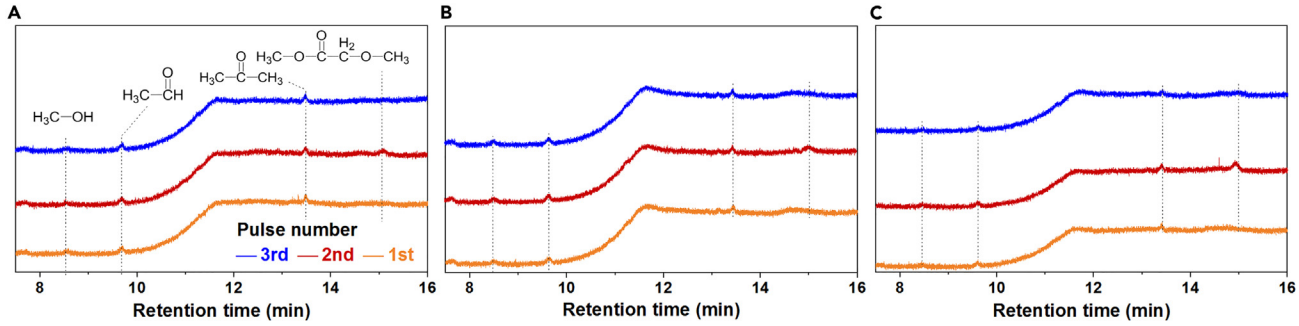

Figure 4. Signals of oxygenated compounds over FID detector during the first 3 O_2 pulses at 500°C

Reaction conditions: pulse injection mode, p = 1 bar, CH_4/O_2 = 2, contact time = 1 ms, pulse interval = 16 min, (A) H_2 pretreatment, (B) O_2 pretreatment, (C) CH_4 pretreatment. Retention time (Rt) of methanol 8.5 min, Rt of aldehyde 9.6 min, Rt of acetone 13.5 min, Rt of methyl methoxyacetate 15.1 min are shown in (A). The signal baseline of different chromatogram was shifted upward along the vertical axis.

compounds under optimized reaction conditions. Gas phase effluents were detected by online MS, and liquid products were simultaneously collected by absorbing the effluent gas in anisole and analyzed by gas chromatograph (C_2Cl_6 was used as the internal standard, shown in transparent methods supplemental file).

Figure 5 shows the measured signals of O_2 (*m/z* 32) and gas phase effluents (H_2 (*m/z* 2), H_2O (*m/z* 18), CO (*m/z* 28) and CO_2 (*m/z* 44)) at different temperatures as a function of time on stream. In the blank experiment at 20°C, only the O_2 signal was detected. Compared with blank experiment, the O_2 signal decreased with the increase of temperature. At 550°C and higher temperature, O_2 signal was almost invisible and the intensity of $CO/CO_2/H_2O$ signals increased rapidly. In the continuous feed mode, the induction period was not observed, which because of the high content of O_2 makes the reaction quickly reaches to a stable state.

The liquid products were analyzed by gas chromatograph and the results are shown in Figure 6. Oxygenated compounds (including methanol, acetaldehyde, propyl aldehydes and acetone) were observed, and their amount increased slightly with the temperature in the range from 400 to 500°C. Much higher amount of acetone (1.19 μmol/h) was detected at 525°C with a sharp decrease with the increasing temperature (550°C, 0.070 μmol/h; 600°C, 0.071 μmol/h), and an increase of methanol amount (550°C, 1.75 μmol/h; 600°C, 1.84 μmol/h). Although methanol is likely to be over-oxidized at these temperatures, the observation of methanol at short contact time (1ms) implies that it could be an intermediate in the CH_4 oxidation. As for other oxygenated compounds, the trend of acetaldehyde formation (400°C, 0.072 μmol/h; 500°C, 0.071 μmol/h; 525°C, 0.086 μmol/h; 550°C, 0.14 μmol/h; 600°C, 0.16 μmol/h) was similar to methanol, while

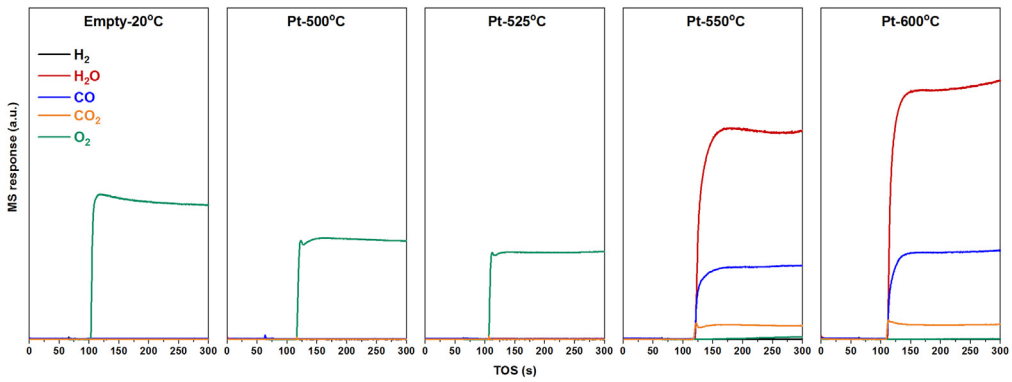

Figure 5. MS spectrum signals of O_2 and gas phase products (CO, CO_2, H_2O and H_2) as a function of time on stream

Reaction conditions: continuous feed mode, p = 1 bar, CH_4/O_2 = 2, contact time = 1 ms, T = 20°C, 500°C, 525°C, 550°C, 600°C.

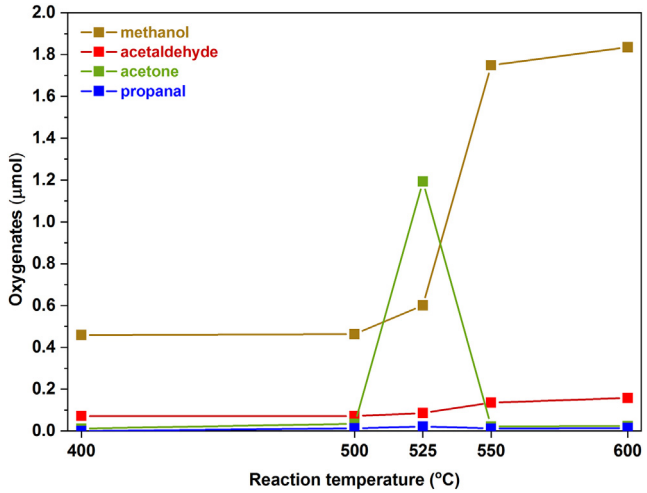

Figure 6. Amount of collected oxygenated compounds (methanol, acetaldehyde, acetone, propyl aldehyde) as a function of reaction temperature

Reaction conditions: continuous feed mode, p = 1 bar, CH_4/O_2 = 2, contact time = 1 ms, T = 400–800°C, TOS = 60 min.

propyl aldehyde (400°C, 0 μmol/h; 500°C, 0.013 μmol/h; 525°C, 0.021 μmol/h; 550°C, 0.012 μmol/h; 600°C, 0.014 μmol/h) was similar to acetone. The similar trends demonstrate that the formation of acetaldehyde might related to methanol and the formation of propyl aldehyde might related to acetone.

Effects of time on stream and contact time on oxygenated intermediates

To probe the mechanism of oxygenated compounds formation, the experiments of different time on stream and contact time at 525°C were conducted under continuous mode. From the results under different time on stream (Figure 7A), we found that most of oxygenated compounds have been generated at the initial stage (the first 1 min), with the methanol of 0.37 μmol and the acetone of 0.77 μmol, respectively. After that time, the amount of the oxygenated compounds changed a little.

The effect of contact time on the oxygenated compounds is shown in Figure 7B. With the decrease of the contact time from 1 ms to 0.28 ms, the amount of methanol decreased from 0.60 μmol to 0.28 μmol, while

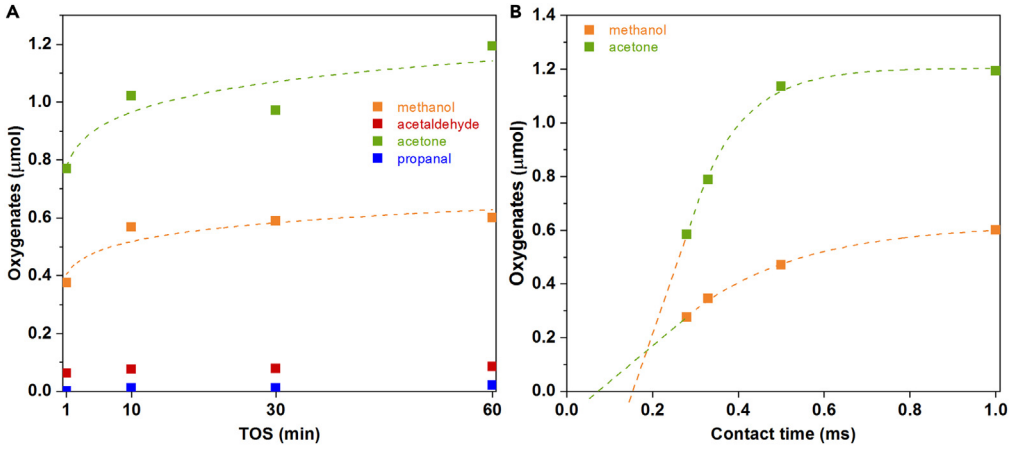

Figure 7. Effects of time on stream and contact time on oxygenated intermediates

Reaction conditions: continuous feed mode, p = 1 bar, CH_4/O_2 = 2, contact time = 1 ms, T = 525°C. (A) amount of oxygenated compounds (methanol, acetaldehyde, acetone and propyl aldehyde) as a function of TOS (1, 10, 30, 60 min); (B) amount of oxygenated compounds (methanol, acetone) as a function of contact time (0.28, 0.33, 0.5, 1 ms).

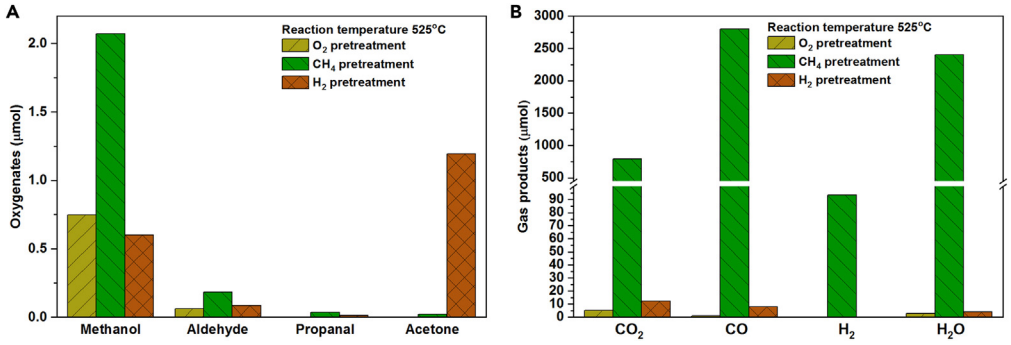

Figure 8. Amount of oxygenated compounds (methanol, acetaldehyde, acetone, propyl aldehyde) and gas products with O_2, CH_4 or H_2 pretreatment

Reaction conditions: continuous feed mode, p = 1 bar, CH_4/O_2 = 2, contact time = 1 ms, T = 525°C, TOS = 60 min. (A) amount of oxygenated compounds; (B) amount of gas products.

the amount of acetone decreased much more remarkably (from 1.19 μmol to 0.58 μmol). To extend the evolution curves of methanol and acetone on Figure 10 to shorter contact time, it could be inferred that methanol formation should be earlier than acetone during CH_4 oxidation, and acetone might derive from methanol. Further research are necessary to verify this assumption.

CH_4 oxidations over Pt catalysts with CH_4, O_2 or H_2 pretreatment were conducted at 525°C in continuous feed mode and the results are shown in Figure 8. Obvious differences were observed in the product distributions. Acetone was the dominated oxygenated compound with H_2 pretreatment, which decreased to 0.035 μmol/h with CH_4 pretreatment and disappeared with O_2 pretreatment. The amount of methanol was 2.07 μmol/h with CH_4 pretreatment, decreased to 0.60 μmol/h with H_2 pretreatment and 0.75 μmol/h with O_2 pretreatment.

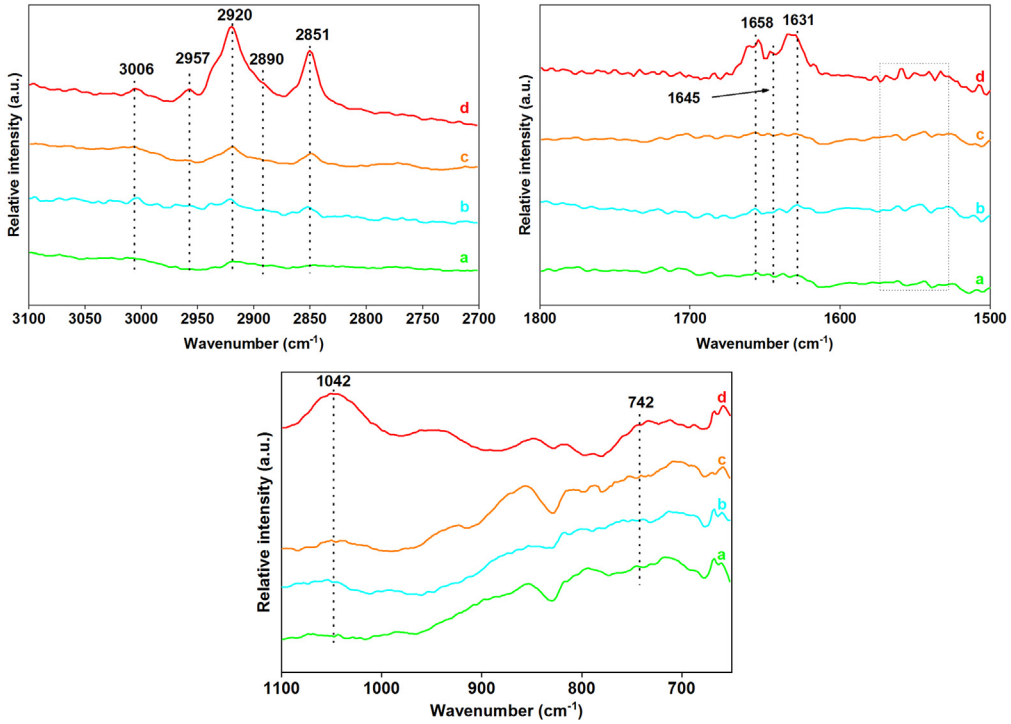

Figure 9. DRIFT spectra of the catalyst recorded after the CH_4 pretreatment

(a) before CH_4 pretreatment, (b) CH_4 pretreatment at 500°C, (c) CH_4 pretreatment at 525°C, (d) CH_4 pretreatment at 600°C.

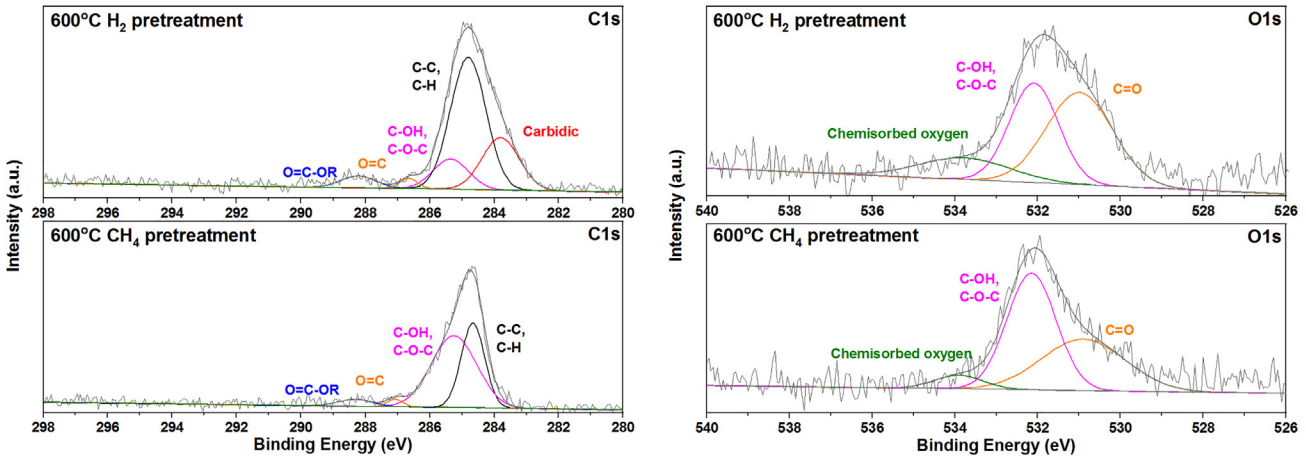

Figure 10. XPS spectra recorded for Pt with CH_4 or H_2 pretreatment at 600°C after the first O_2 pulse

Reaction conditions: p = 1 bar, T = 525°C, with H_2 and CH_4 pretreatment respectively at 600°C for 30 min. As for H_2 pretreatment experiment, CH_4 stream was pre-introduced for 10 min at 525°C before O_2 pulse for stability of the reaction system.

The change of gas products was similar to the pulse injection mode, CH_4 pretreatment led to a significantly increase of the activity and a large amount of gas products were generated (the MS spectra signals are given in Figure S8). These results indicate that Pt surface pretreated by CH_4 provides new active intermediate species for CH_4 oxidation, which might consist of alkyl groups and unsaturated bonds, and greatly change the formation route of the oxygenated compounds (mainly methanol) and gas products. Therefore, adjusting the surface state of Pt catalyst by gas pretreatment was demonstrated being an effective way to influence the CH_4 oxidation.

Investigation of intermediate species with methane pretreatment over Pt surface

To illustrate the effect of the intermediates formed during CH_4 pretreatment, detailed experiments were designed to analyze the gas effluents and intermediate species formed on Pt catalysts. The H_2 signal baseline of online MS spectra given in Figure S9 increased more obviously with the increase of temperature, especially at 600°C. This indicates that the significant CH_4 dehydrogenation on Pt surface occurred at 600°C, which would further generate surface hydrocarbon species with saturated or unsaturated bonds.

These surface intermediate species were further investigated by the DRIFT micro-spectroscopy. Corresponding ligands of Pt^0 (with H_2 pretreatment at 600°C) and Pt with CH_4 pretreatment (at 500°C, 525°C and 600°C, respectively) are shown in Figure 9, where IR signals were collected over the Pt wire surfaces. Multiple positive peaks are detected in the range of 2700–3100 cm^{-1} and 1200–1800 cm^{-1} after CH_4 pretreatment. The bands at 2800–3100 cm^{-1} are assigned to the C-H stretching of the aliphatic chain.[27] The peaks at 2920 and 2851 cm^{-1} are attributed to the CH_2.[27–29] The bands at 3006, 2957 and 2890 cm^{-1} are assigned to C-H of CH_4, CH_3 and CH, respectively.[30] An obvious increase in the intensity of these peaks with increasing temperature (from 500°C to 600°C) demonstrates that species with unsaturated bonds were more abundant on Pt surface during CH_4 pretreatment at 600°C. Meanwhile, the bands at 1658, 1645 and 1631 cm^{-1} are assigned to the vibrations of C=C in alkene and H_2O molecules.[27,31,32] The C=C stretching of the aromatic ring was barely visible at 1500–1600 cm^{-1}, but the weak stretching indicates that CH_4 pretreatment could form a small amount of aromatic hydrocarbons on the Pt surface. The bands at 742 cm^{-1} and 1042 cm^{-1} are assigned to Pt-C stretch and the ethene-asymmetric CH_2 wagging mode,[33] which were very visible after CH_4 pretreatment at 600°C. These features demonstrate that the Pt-C bonds and unsaturated intermediates are readily generated over Pt surface in CH_4 atmosphere at high temperature. The formation of Pt-C might provide active sites over Pt surface for subsequent oxidation reaction.

XPS spectra for the surface intermediate species with CH_4 or H_2 pretreatment after the first O_2 pulse was shown in Figure 10. Curve fitting of the C1s and O1s spectra was performed using a Gaussian peak shape. In C1s XPS spectra, the binding energy of the C-C and C-H bonding are assigned at 284.6–285 eV. The chemical shifts of +1.0, +2.5 and +4.0 eV are assigned for the C-OH, C=O and O=C-OH functional groups, respectively.[34,35] Compared with H_2 pretreatment, a peak at 283.6 eV disappeared with CH_4 pretreatment,

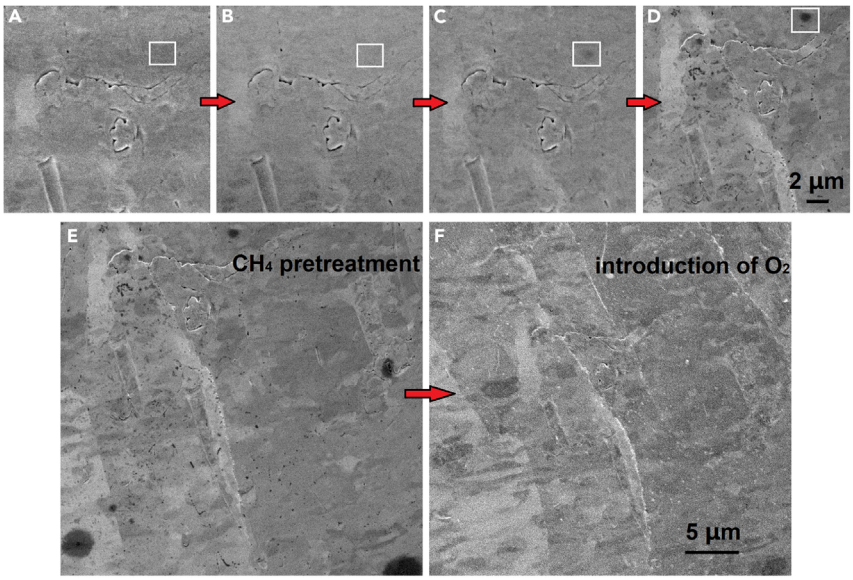

Figure 11. *In situ* ESEM images of the Pt foil with CH_4 pretreatment and the introduction of O_2

(A–F) Local region: CH_4 pretreatment temperature, (A) RT, (B) 500°C, (C) 550°C, (D) 600°C. Enlarged region: (E) CH_4 pretreatment at 600°C, (F) CH_4 was vented and then O_2 was introduced for 10 min.

which is assigned to the carbidic carbon species.[34] In the case of CH_4 pretreatment, the peak at 285.6 eV became broader and increased in intensity and the peak at 284.6 eV became narrow and reduced in intensity. This indicates that more intermediates on Pt surface with CH_4 pretreatment interact with O_2 to form the species containing hydroxyl. Therefore, in the case of H_2 pretreatment, the activity of the carbon species (at 283.6 eV) generated after CH_4/O_2 pulse might be low and difficult to react with O_2.

In O1s XPS spectra, the chemical shifts of 530.5–530.9, 532–532.3, 534–534.2 eV are assigned to the C=O, C-OH (C-O-C) and chemisorbed oxygen functional groups, respectively.[34,35] These spectra were consistent with the results that methanol was the most numerous oxygenate at the initial of CH_4 oxidation after CH_4 pretreatment. Compared with H_2 pretreatment, chemisorbed oxygen was less with CH_4 pretreatment suggesting that more O atom was incorporated in the products during the reaction. Combined with these results, the active intermediate species with unsaturated bonds generated on Pt surface after CH_4 pretreatment at high temperature, and then O_2 readily interacts with these active species to generate hydroxyl groups instead of forming chemisorbed oxygen.

In situ ESEM study for the methane pretreatment and the introduction of oxygen over Pt surface

ESEM was used to observe the Pt surface state *in-situ* during CH_4 pretreatment and the introduction of O_2. *In situ* ESEM images under a pure CH_4 atmosphere of 100 Pa from room temperature (RT) to 600°C are shown in Figures 11A–11D. Darker contrast circular spots appeared at some regions on the Pt foil with the temperature increased to 550°C, and at 600°C, circular spots were clearly visible. The generation of intermediate species on the Pt surface with CH_4 pretreatment was observed. As shown in Figures 11E and 11F, the brightness and contrast of these circular spots were weakened when CH_4 was vented and then O_2 was introduced, meanwhile, a large number of bright small spots were observed. These observations indicate that the intermediate species is readily reacted with the O_2 and then further transform to other products.[36]

Reaction mechanism of the induction period during the methane oxidation over Pt-based catalyst

Based on the experimental results and discussion, a plausible mechanism of the induction period during the CH_4 oxidation was proposed (Figure 12). First, CH_4 is adsorbed on Pt surface and dehydrogenated to form methyl group. After that, partial methyl groups undergo further dehydrogenation, whereas others react with O_2 to form methoxy groups and then interact with surface hydroxyl groups to form methanol. The

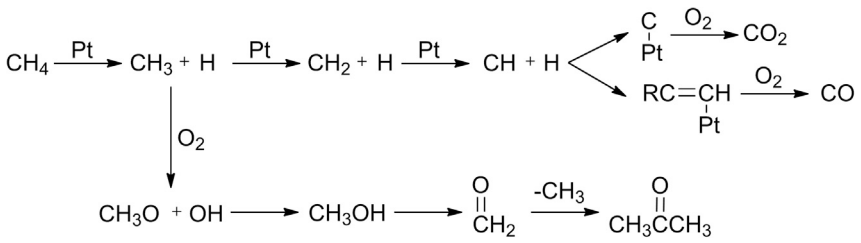

Figure 12. Proposed mechanism for the methane oxidation over Platinum

accumulation of methyl, methylene and methine groups is the reason for the formation of the induction period. With the increasing temperature, the dehydrogenation is accelerated and more intermediate species containing unsaturated C=C bonds can be formed during the accumulation process. These unsaturated intermediates are more active and provide active sites for the oxidation reaction, resulting in a shortened induction period. Meanwhile, methanol undergoes dehydrogenation to form a formaldehyde intermediate, which rapidly interacts with the methyl groups to form acetone.

Conclusions

In summary, the CH_4 oxidation over Pt wires catalyst was systematically studied in a specially designed capillary reactor under the condition of very short contact time ($\leq$1 ms). For the first time, we found an induction period at the initial stage of CH_4 oxidation. The CH_4 oxidation initiates from the interaction of CH_4 and Pt to generate methyl group and methylene group. Methyl group and methylene group with low catalytic activity need to accumulate to react with O_2, which leads to the formation of induction period. Pt-C active sites and unsaturated intermediates are more readily to be generated on the Pt surface after CH_4 pretreatment at high temperature, which greatly shorten the induction period. Multiple oxygenated compounds were detected and the distribution of oxygenated compounds is correlated with the temperature and contact time. CH_4 pretreatment at high temperature could also greatly change the distribution of oxygenated compounds, and a significant increase in methanol might be beneficial to shorten the induction period. This work provides a new insight for the research of CH_4 oxidation.

Limitations of the study

Catalyst mounting of the self-designed capillary reactor is relatively difficult and limited by the inner diameter of reactor, and the *in-situ* characterization on the catalyst in the capillary is difficult. Future work is required to improve the filling method of the catalyst, so that more characterization methods can be applied to this reaction system.

STAR★METHODS

Detailed methods are provided in the online version of this paper and include the following:

- KEY RESOURCES TABLE
- RESOURCE AVAILABILITY
  - Lead contact
  - Materials availability
  - Data and code availability
- METHOD DETAILS
  - General reagent information
  - Reaction system
  - Calculation of conversion and selectivity
  - Catalyst characterization
- QUANTIFICATION AND STATISTICAL ANALYSIS
- ADDITIONAL RESOURCES

SUPPLEMENTAL INFORMATION

Supplemental information can be found online at https://doi.org/10.1016/j.isci.2023.107061.

ACKNOWLEDGMENTS

This work was supported by the National Natural Science Foundation of China (grant nos. 21991093, 21991090). *In-situ* ESEM experiments were carried out on the Quanta 650 (Thermo Scientific Company) in the electron microscopy center at the Dalian Institute of Chemical Physics of Chinese Academy of Sciences.

AUTHOR CONTRIBUTIONS

K.Y. conceived and performed the experiments, collected and analyzed the data, and wrote the manuscript. J.L. analyzed the data and revised the manuscript. Z.Z. analyzed the data and discussion. Z.L. supervised the study, designed the experiments and revised the manuscript. All authors discussed the results and commented on the manuscript at all stages.

DECLARATION OF INTERESTS

The authors declare no competing interests.

Received: March 2, 2023
Revised: March 30, 2023
Accepted: June 2, 2023
Published: June 8, 2023

REFERENCES

1. Sher Shah, M.S.A., Oh, C., Park, H., Hwang, Y.J., Ma, M., and Park, J.H. (2020). Catalytic oxidation of methane to oxygenated products: recent advancements and prospects for electrocatalytic and photocatalytic conversion at low temperatures. Adv. Sci. *7*, 2001946. https://doi.org/10.1002/advs.202001946.

2. Schwach, P., Pan, X., and Bao, X. (2017). Direct conversion of methane to value-added chemicals over heterogeneous catalysts: challenges and prospects. Chem. Rev. *117*, 8497–8520. https://doi.org/10.1021/acs.chemrev.6b00715.

3. Pitchai, R., and Klier, K. (1986). Partial oxidation of methane. Catal. Rev. *28*, 13–88. https://doi.org/10.1080/03602458608068085.

4. Ashcroft, A.T., Cheetham, A.K., Green, M.L.H., and Vernon, P.D.F. (1991). Partial oxidation of methane to synthesis gas-using carbon-dioxide. Nature *352*, 225–226. https://doi.org/10.1038/352225a0.

5. Vernon, P.D.F., Green, M.L.H., Cheetham, A.K., and Ashcroft, A.T. (1990). Partial oxidation of methane to synthesis gas. Catal. Lett. *6*, 181–186. https://doi.org/10.1007/Bf00774718.

6. Tao, F.F., Shan, J.J., Nguyen, L., Wang, Z., Zhang, S., Zhang, L., Wu, Z., Huang, W., Zeng, S., and Hu, P. (2015). Understanding complete oxidation of methane on spinel oxides at a molecular level. Nat. Commun. *6*, 7798. https://doi.org/10.1038/ncomms8798.

7. Popescu, I., Tanchoux, N., Tichit, D., and Marcu, I.-C. (2017). Total oxidation of methane over supported CuO: influence of the Mg x Al y O support. Appl. Catal. Gen. *538*, 81–90. https://doi.org/10.1016/j.apcata.2017.03.012.

8. Feng, S., Yang, W., and Wang, Z. (2011). Synthesis of porous NiFe2O4 microparticles and its catalytic properties for methane combustion. Mater. Sci. Eng., B *176*, 1509–1512. https://doi.org/10.1016/j.mseb.2011.09.007.

9. Geng, H., Yang, Z., Ran, J., Zhang, L., Yan, Y., and Guo, M. (2015). Low-concentration methane combustion over a Cu/γ-Al2O3 catalyst: effects of water. RSC Adv. *5*, 18915–18921. https://doi.org/10.1039/c5ra00633c.

10. Geng, H., Yang, Z., Zhang, L., Ran, J., Yan, Y., and Guo, M. (2016). Effects of O2/CH4 ratio on methane catalytic combustion over Cu/γ-Al2O3 particles. Int. J. Hydrogen Energy *41*, 18282–18290. https://doi.org/10.1016/j.ijhydene.2016.08.134.

11. Zhang, Y., Qin, Z., Wang, G., Zhu, H., Dong, M., Li, S., Wu, Z., Li, Z., Wu, Z., Zhang, J., et al. (2013). Catalytic performance of MnOx–NiO composite oxide in lean methane combustion at low temperature. Appl. Catal. B Environ. *129*, 172–181. https://doi.org/10.1016/j.apcatb.2012.09.021.

12. Lim, T.H., Cho, S.J., Yang, H.S., Engelhard, M.H., and Kim, D.H. (2015). Effect of Co/Ni ratios in cobalt nickel mixed oxide catalysts on methane combustion. Appl. Catal. Gen. *505*, 62–69. https://doi.org/10.1016/j.apcata.2015.07.040.

13. Yan, Q. (2004). Partial oxidation of methane to H2 and CO over Rh/SiO2 and Ru/SiO2 catalysts. J. Catal. *226*, 247–259. https://doi.org/10.1016/j.jcat.2004.05.028.

14. Oh, S., Mitchell, P.J., and Siewert, R.M. (1991). Methane oxidation over alumina-supported noble-metal catalysts with and without cerium additives. J. Catal. *132*, 287–301. https://doi.org/10.1016/0021-9517(91)90149-X.

15. Mhadeshwar, A.B., and Vlachos, D.G. (2007). A catalytic reaction mechanism for methane partial oxidation at short contact times, reforming, and combustion, and for oxygenate decomposition and oxidation on platinum. Ind. Eng. Chem. Res. *46*, 5310–5324. https://doi.org/10.1021/ie070322c.

16. Cullis, C., and Willatt, B.M. (1983). Oxidation of methane over supported precious metal-catalysts. J. Catal. *83*, 267–285. https://doi.org/10.1016/0021-9517(83)90054-4.

17. Hickman, D.A., and Schmidt, L.D. (1993). Production of syngas by direct catalytic-oxidation of methane. Science *259*, 343–346. https://doi.org/10.1126/science.259.5093.343.

18. Hickman, D.A., Haupfear, E.A., and Schmidt, L.D. (1993). Synthesis gas-formation by direct oxidation of methane over Rh monoliths. Catal. Lett. *17*, 223–237. https://doi.org/10.1007/Bf00766145.

19. Hickman, D., and Schmidt, L.D. (1992). Synthesis gas-formation by direct oxidation of methane over Pt monoliths. J. Catal. *138*, 267–282. https://doi.org/10.1016/0021-9517(92)90022-A.

20. Au, C.T., and Wang, H.Y. (1997). Mechanistic studies of methane partial oxidation to syngas over SiO2-supported rhodium catalysts. J. Catal. *167*, 337–345. https://doi.org/10.1006/jcat.1997.1609.

21. Heitnes, K., Lindberg, S., Rokstad, O.A., and Holmen, A. (1995). Catalytic partial oxidation of methane to synthesis gas. Catal. Today *24*, 211–216. https://doi.org/10.1016/0920-5861(95)00027-D.

22. Ashcroft, A.T., Cheetham, A.K., Foord, J.S., Green, M.L.H., Grey, C.P., Murrell, A.J., and Vernon, P.D.F. (1990). Selective oxidation of methane to synthesis gas-using

transition-metal catalysts. Nature *344*, 319–321. https://doi.org/10.1038/344319a0.

23. Dissanayake, D., Rosynek, M.P., Kharas, K.C.C., and Lunsford, J.H. (1991). Partial oxidation of methane to carbon-monoxide and hydrogen over a Ni/Al2o3 catalyst. J. Catal. *132*, 117–127. https://doi.org/10.1016/0021-9517(91)90252-Y.

24. Chang, Y.F., and Heinemann, H. (1993). Partial oxidation of methane to syngas over Co/mgo catalysts - is it low-temperature. Catal. Lett. *21*, 215–224. https://doi.org/10.1007/Bf00769473.

25. Mallens, E.P.J., Hoebink, J.H.B.J., and Marin, G.B. (1995). An investigation on the reaction-mechanism for the partial oxidation of methane to synthesis gas over platinum. Catal. Lett. *33*, 291–304. https://doi.org/10.1007/Bf00814232.

26. Persson, K., Jansson, K., and Jaras, S. (2007). Characterisation and microstructure of Pd and bimetallic Pd–Pt catalysts during methane oxidation. J. Catal. *245*, 401–414. https://doi.org/10.1016/j.jcat.2006.10.029.

27. Nair, S.A., Nozaki, T., and Okazaki, K. (2007). In situ fourier transform infrared (FTIR) study of nonthermal-plasma-assisted methane oxidative conversion. Ind. Eng. Chem. Res. *46*, 3486–3496. https://doi.org/10.1021/ie0606688.

28. Reinke, P., Jacob, W., and Möller, W. (1993). Influence of the ion energy on the growth and structure of thin hydrocarbon films. J. Appl. Phys. *74*, 1354–1361. https://doi.org/10.1063/1.354892.

29. Deschenaux, C., Affolter, A., Magni, D., Hollenstein, C., and Fayet, P. (1999). Investigations of CH4, C2H2 and C2H4 dusty RF plasmas by means of FTIR absorption spectroscopy and mass spectrometry. J. Phys. D Appl. Phys. *32*, 1876–1886. https://doi.org/10.1088/0022-3727/32/15/316.

30. Berndt, J., Hong, S., Kovačević, E., Stefanović, I., and Winter, J. (2003). Dust particle formation in low pressure Ar/CH4 and Ar/C2H2 discharges used for thin film deposition. Vacuum *71*, 377–390. https://doi.org/10.1016/S0042-207x(02)00767-4.

31. Allen, N.S., Edge, M., Rodriguez, M., Liauw, C.M., and Fontan, E. (2001). Aspects of the thermal oxidation, yellowing and stabilisation of ethylene vinyl acetate copolymer. Polym. Degrad. Stabil. *71*, 1–14.

32. Busca, G., Finocchio, E., Lorenzelli, V., Trombetta, M., and Rossini, S.A. (1996). IR study of alkene allylic activation on magnesium ferrite and alumina catalysts. Faraday Trans. *92*, 4687–4693. https://doi.org/10.1039/ft9969204687.

33. Wensink, F.J., Roos, N., Bakker, J.M., and Armentrout, P.B. (2022). C-H bond activation and C-C coupling of methane on a single cationic platinum center: a spectroscopic and theoretical study. Inorg. Chem. *61*, 11252–11260. https://doi.org/10.1021/acs.inorgchem.2c01328.

34. Biniak, S., Szymański, G., Siedlewski, J., and Świątkowski, A. (1997). The characterization of activated carbons with oxygen and nitrogen surface groups. Carbon *35*, 1799–1810. https://doi.org/10.1016/S0008-6223(97)00096-1.

35. Yang, D., Velamakanni, A., Bozoklu, G., Park, S., Stoller, M., Piner, R.D., Stankovich, S., Jung, I., Field, D.A., Ventrice, C.A., and Ruoff, R.S. (2009). Chemical analysis of graphene oxide films after heat and chemical treatments by X-ray photoelectron and Micro-Raman spectroscopy. Carbon *47*, 145–152. https://doi.org/10.1016/j.carbon.2008.09.045.

36. Barroo, C., Wang, Z.J., Schlögl, R., and Willinger, M.G. (2019). Imaging the dynamics of catalysed surface reactions by in situ scanning electron microscopy. Nat. Catal. *3*, 30–39. https://doi.org/10.1038/s41929-019-0395-3.

STAR★METHODS

KEY RESOURCES TABLE

REAGENT or RESOURCE	SOURCE	IDENTIFIER
Chemicals, peptides, and recombinant proteins		
Pt wires	Sigmund Cohn	CAS 7440-06-4
Pt foil	Alfa Aesar	CAS 7440-06-4
C_7H_8O	Aladdin	CAS 100-66-3
C_2Cl_6	Aladdin	CAS 67-72-1
CH_4	Dalian Special Gases	CAS 74-82-8
He	Dalian Special Gases	CAS 7440-59-7
O_2	Dalian Special Gases	CAS 132259-10-0
Critical commercial assays		
On-line gas chromatograph	Agilent	7890B
On-line mass spectroscopy	PFEIFFER	Omnistar GSD320
Software and algorithms		
OriginPro 2020	OriginLab Corporation	Massachusetts, USA
ChemDraw Professional	PerkinElmer	https://www.perkinelmer.com/category/chemdraw
Other		
X-ray photoelectron spectroscopy	Thermo Fisher Scientific	Escalab 250Xi
Fourier transform infrared spectroscopy	Bruker	VERTEX 70v
In-situ ESEM	Thermo Fisher Scientific	FEI Quanta 650

RESOURCE AVAILABILITY

Lead contact

Further information and requests for resources should be directed to and will be fulfilled by the lead contact, Professor Zhongmin Liu (liuzm@dicp.ac.cn).

Materials availability

No new materials were generated in this study, and all reagents were commercially available and used without purification.

Data and code availability

- The published article includes all datasets generated or analyzed during this study.
- Any additional information required to reanalyze the data reported in this paper is available from the lead contact upon request.
- This paper does not report original code.

METHOD DETAILS

General reagent information

The platinum wires with 0.05 mm diameter. Methane (20 % in volume, containing 80 % helium as the balance, 99.9 % purity), oxygen (50 % in volume, containing 50 % helium as the balance, 99.9 % purity) and helium (99.9 % purity).

Reaction system

CH_4 oxidation was investigated with a quartz capillary reactor (0.5 mm inner diameter) which was held in place by stainless steel jointing with graphite gaskets sealing. Typically, 1 cm (8 mg) of the Pt wires was packed in the reactor. The reactor was placed into the electric furnace, which had a 2 cm long constant

temperature zone. The reaction temperature (400~800°C) was measured by a K-type thermocouple attached tightly to the outer wall of the reactor. The Pt wire catalyst were pre-reduced *in situ* in flowing mixture of H_2 and helium (30 ml/min) for 30 minutes at 600°C. The reactions were carried out under atmospheric pressure and the feed gas (total flow rate, 60 ml/min) ratio was CH_4/O_2/He = 2/1/9. Flow rates were controlled by electronic flow controllers (Beijing Seven-star Electronic Technology Co., Ltd).

All the effluent products were analyzed by an online mass spectrometer and an online gas chromatograph (Agilent 7890B) equipped with Agilent Poraplot Q-HT capillary column (25 m × 0.32 mm × 10 μm) connected to a flame ionization detector (FID).

The capillary micro-reactor was connected to a special designed inlet system by modifying the valves of Agilent 7890 B gas chromatograph (Figures S10 and S11), which enabled the reactions could be operated either in continuous feed mode or in pulse injection mode. In the case of pulse injection mode, the pretreating gas was directly introduced into the reactor through the six-way valve of GC, while the mixture of oxygen and helium (O_2 ~ 50%, He ~ 50%) constantly filled the loop (250 μl) of the valve. When the six-way valve was switched through the control system of GC, the gas mixture in the sample loop was injected into the flowing gas (50 ml/min, CH_4 ~ 20%, He ~ 80%) using helium carrier gas (10 ml/min). The outlet of the reactor connected to the other ten-way valve which either delivered the effluent to GC for analysis or as vented gas. The pulse reaction interval was 16 min and the mixture of methane and helium continuously flowed through the Pt wire catalyst during the interval. Before the first pulse of O_2, CH_4 stream was pre-introduced for ~10 min to stabilize the online mass spectrometer.

In the case of continuous feed mode, the mixture of O_2 and helium was introduced into the CH_4 stream by switching the six-way valve and flowed into the reactor. After reaction, the valve was switched back. Oxygenated compounds were collected by absorbing the effluent gas in anisole with C_2Cl_6 (100 ppm) as an internal standard. The outlet of the capillary micro-reactor was directly inserted into the bottom of the centrifugal tube with 5 g absorption solvent, which was analyzed by GC after the reaction.

Calculation of conversion and selectivity

The conversion and selectivity were calculated as follows:

$$Con_{CH_4} = \frac{CH_{4\,inlet} - CH_{4\,outlet}}{CH_{4\,inlet}} * 100\%$$

$$Sel_{products} = \frac{products_{outlet}}{\sum_1^n products_{outlet}} * 100\%$$

Where CH_{4inlet}, $CH_{4outlet}$ and $products_{outlet}$ represent moles fraction of CH_4 and products at the inlet and the outlet, respectively. $\sum_1^n products_{outlet}$ represents the sum of the mole fractions of all products at the outlet. CH_4 conversion and product selectivity were calculated based on the above equation by MS spectrum results. The mole fractions of CH_4 and gas products were calculated based on the MS response signals (CH_4 ~ m/z 15, CO ~ m/z 28, CO_2 ~ m/z 44, H_2 ~ m/z 2, H_2O ~ m/z 18) which was calibrated by standard gas (containing CH_4, O_2, He, CO, CO_2, H_2 and H_2O).

Catalyst characterization

X-ray photoelectron spectroscopy (XPS) was measured on a Thermos ESCALAB 250Xi using a monochromatic Al*K*α X-ray source (1486 eV, 15 KV, 10.8 mA). The surface atomic ratio was determined from the peak areas of O1s, C1s and Pt4f, respectively.

Diffuse reflectance infrared Fourier transform spectroscopy (DRIFT) micro-spectroscopy were collected on a Bruker Vertex 27 spectroscope supplied with MCT detector. Before characterization, Pt wires with 0.05mm in diameter and 2 cm in length were pretreated in CH_4 effluent at 500°C, 525°C and 600°C for 30 min, respectively.

In-situ environmental scanning electron microscopy (ESEM) was performed in a commercial ESEM (FEI Quanta 650) equipped with a commercial heating stage and He, CH_4, O_2 feeding unit. The accelerating

voltage was 20 kV with an objective lens aperture of 30 μm. The high magnification imaging (×20000) was conducted when the temperature is stable for 10 minutes.

QUANTIFICATION AND STATISTICAL ANALYSIS

Figures were analyzed by Origin from the raw data.

ADDITIONAL RESOURCES

This work does not include any additional resources.